



## Biogenic Synthesis, Characterization, and Evaluation of Larvicidal and Antibacterial Activities of Zinc Oxide Nanoparticles using *Paspalum vaginatum* Extract

Henry U. Anuforo<sup>1,2\*</sup>, Priscilla N. Abara<sup>1</sup>, Ethelbert U. Ezeji<sup>2</sup>, Campbell O. Akujobi<sup>3</sup>, Nneamaka A. Chiegboka<sup>1</sup>, Angela C. Udebuani<sup>2</sup>, Olusola O. Ibeh<sup>4</sup>, Toochukwu E. Ogbulie<sup>2</sup>

<sup>1</sup>Department of Biology, School of Biological Sciences, Federal University of Technology, PMB 1526, Owerri, Nigeria

<sup>2</sup>Department of Biotechnology, School of Biological Sciences, Federal University of Technology, PMB 1526, Owerri, Nigeria

<sup>3</sup>Department of Microbiology, School of Biological Sciences, Federal University of Technology, PMB 1526, Owerri, Nigeria

<sup>4</sup>Department of Forensic Science, School of Biological Sciences, Federal University of Technology, PMB 1526, Owerri, Nigeria

### ARTICLE INFO

#### Article history:

Received 20 July 2025

Revised 29 July 2025

Accepted 19 August 2025

Published online 01 December 2025

**Copyright:** © 2025 Anuforo *et al* This is an open-access article distributed under the terms of the [Creative Commons Attribution License](#), which permits unrestricted use, distribution, and reproduction in any medium, provided the original author and source are credited.

### ABSTRACT

The advantages of biological method of nanoparticle synthesis over chemical and physical methods cannot be overemphasized. However, its sustainability depends on the continuous availability of extracts used as reducing and capping agents. To prevent over-exploitation of a few plant sources for this, there is a need to increase available sources of suitable extracts. This study aimed to biogenically synthesize, characterize, and evaluate the larvicidal and antibacterial activities of zinc oxide nanoparticles using *Paspalum vaginatum* extract. Phytochemical assessment of the aqueous extract was done using gas chromatography–mass spectrometry (GC-MS) before zinc oxide nanoparticles (ZnONPs) biosynthesis using 0.05 M zinc nitrate hexahydrate. Following their characterization with Fourier transform infrared spectroscopy, X-ray diffraction (XRD) analysis, dynamic light scattering, ultraviolet-visible spectroscopy, and transmission electron microscopy, the antibacterial and larvicidal activities of the resulting ZnONPs were assayed. Results showed structures of ten (10) components of the extract. The XRD spectrum indicated the crystalline nature of synthesized ZnONPs, with hexagonal wurtzite structure. Their maximum absorbance of ultraviolet visible light occurred at 307 nm. Micrograph revealed their spherical shapes, with a mean size of  $3.96 \pm 2.4$  nm. Also, there was appreciable dose- and time-dependent larvicidal activity of synthesized ZnONPs against instar IV *Anopheles* sp larvae, with  $88.3 \pm 0.0\%$  mortality recorded after 26 h of exposure. At  $53.3$   $\mu\text{g/mL}$ , synthesized ZnONPs recorded  $11.33 \pm 7.2$  mm and  $6.0 \pm 2.2$  mm growth inhibitions against *Salmonella* spp. and *Escherichia coli*, respectively. Results of this study confirm that *P. vaginatum* aqueous extract is suitable for the synthesis of ZnONPs with considerable antibacterial and larvicidal activities.

**Keywords:** Nanoparticles, Phytochemical composition, Larvicidal activity, Biosynthesis, *Paspalum vaginatum*, Plant extract.

### Introduction

Globally, mosquitoes have remained vectors of public health importance because they transmit different communicable diseases.<sup>1</sup> One of the life-threatening diseases is malaria, caused by *Plasmodium*, and transmitted by female *Anopheles* mosquitoes. In over ninety countries, malaria has continued to pose serious health challenges. With over 219 million people living in malaria-prone areas, it is estimated that globally, it causes about 1.1 to 2.7 million deaths annually.<sup>2</sup> The chemical method of controlling mosquito populations involves the use of synthetic insecticides, such as pyrethroids, organophosphates (temephos, methoprene), insect growth regulators, and bacterial insecticides.<sup>1,3</sup> However, indiscriminate and continuous applications of the same insecticides have resulted in the development of resistance in mosquitoes, as well as other insect pests.<sup>1,4,5</sup>

\*Corresponding author; Email: [henry.anuforo@futo.edu.ng](mailto:henry.anuforo@futo.edu.ng)  
Tel.: +234(0)8066583404

**Citation:** Anuforo H U, Abara P N, Ezeji E U, Akujobi C O, Chiegboka N A, Udebuani A C, Ibeh O O, Ogbulie T E. Biogenic Synthesis, Characterization, and Evaluation of Larvicidal and Antibacterial Activities of Zinc Oxide Nanoparticles using *Paspalum vaginatum* Extract. Trop J Nat Prod Res. 2025; 9(11): 5828 – 5838 <https://doi.org/10.26538/tjnpr/v9i11.75>

Official Journal of Natural Product Research Group, Faculty of Pharmacy, University of Benin, Benin City, Nigeria.

These synthetic substances are also harmful to the environment and other non-target organisms.<sup>6</sup> Consequently, the development and use of alternative, eco-friendly methods, such as biopesticides and secondary metabolites, are urgently needed to combat ravaging resistance in mosquito species.<sup>7</sup> Nanobiotechnology refers to an emerging aspect of biology, which involves the application of nanomaterials, including silver (Ag), gold (Au), copper (Cu), aluminum (Al), iron (Fe), cobalt (Co), zinc (Zn), etc., in diverse biological systems.<sup>8</sup> Nanoparticles are materials with at least one dimension measured between 1 to 100 nm, which gives them special, improved chemical and physical properties, compared to their bulk.<sup>9</sup> Because nanomaterials are cheap and do not involve harmful substances, their application is considered one of the modern promising methods in mosquito control. Studies have proven that at very low concentrations, many nanoparticles have shown activity against different mosquito species.<sup>10</sup> Among others, zinc oxide nanoparticles (ZnONPs) have witnessed increasing applications in different sectors.<sup>11</sup> This is due to its biodegradability, high ultraviolet ray absorption, and low toxicity to humans and other higher animals. Its capability to serve as a good surface material makes it useful in the biomedical field.<sup>8</sup> ZnONPs possess high toxicity against microorganisms and high stability under extreme processing conditions. Thus, they are used in different fields as antimicrobial

agents.<sup>1</sup> They have shown appreciable antibacterial activities against diverse bacterial isolates, including *Staphylococcus aureus*, *Escherichia coli*,<sup>12</sup> *Bacillus subtilis*, as well as antifungal activity against *Aspergillus flavus*, *Alternaria alternata*.<sup>13</sup>

ZnONPs are synthesized through several physical, chemical and biological methods. However, physical methods are limited by their expensive nature, while chemical methods are not biocompatible and eco-friendly. Only biosynthesis is “green,” cheap and biocompatible.<sup>14</sup> Use of plant extracts is one of the sustainable biological methods of synthesizing nanoparticles.<sup>15</sup> Most importantly, the preference for ZnONPs, and other nanoparticles, is hinged on the eco-friendliness and cost-effectiveness of the method of their synthesis, coupled with the biocompatibility of the resulting nanoparticles.

An extensive review of studies revealed that most previous works involved extracts from plants that either have economic, edible or medicinal relevance. For instance, reports have indicated the use of leaf extract of *Azadirachta indica*,<sup>16</sup> *Zea mays* leaf extract,<sup>17</sup> *Hibiscus rosa sinensis* extract,<sup>18</sup> *Aloe vera* leaf extract,<sup>19</sup> leaf extract of *Catharanthus roseus*,<sup>20</sup> and leaf extract of *Coffea arabica*,<sup>21</sup> to biosynthesize zinc oxide nanoparticles. These studies have proven the efficacy of ZnONPs synthesized from plant extracts against some bacterial isolates and other target organisms. However, we think that there may be an increased risk of overexploitation of these plants, should sourcing of extracts for utilization in the field of nanotechnology be limited to them. Thus, to guarantee the sustainable application of the biological method of synthesizing nanoparticles, there is a need to diversify the sources of reducing and capping agents, away from these economically and medically useful plant materials. Thus, this study aimed to evaluate the larvicidal and antibacterial activities of zinc oxide nanoparticles synthesized using *Paspalum vaginatum* extract. *P. vaginatum*, being an underutilized grass species, offers a promising alternative source of plant extract, contributing to the diversification of sources and preventing over-exploitation. This contextual review informs the research question: Can biogenic synthesis of zinc oxide nanoparticles using *P. vaginatum* extract provide a sustainable alternative to over-exploited plant species, contributing to the conservation of biodiversity?

Thus, the use of *P. vaginatum* extract for the synthesis of ZnONPs, as well as its applications against selected bacterial isolates and mosquito larvae, which have not been reported in previous studies, is novel. The research method adopted in this study was due to its ability to ensure high-quality data collection, credibility, and generalizability, thereby directly contributing to the study's overall impact and relevance.

## Material and Methods

All reagents including zinc nitrate hexahydrate ( $\text{Zn}(\text{NO}_3)_2 \cdot 6\text{H}_2\text{O}$ ) (Axiom Chemicals Pvt. Ltd, India with 98%), sodium hydroxide (NaOH) pellets (Annexe Chem Pvt. Ltd. India with 99% purity), hydrochloric acid (HCl) (Yujiang Chemical Co., Ltd., China with 98% purity) and bacterial media (Shanghai Fine Biotech Co., Ltd, China) used in this study are analytical grades. These were purchased from known commercial suppliers and used without further purification.

### Collection and plant sample preparation

Healthy *Paspalum vaginatum* leaf samples were obtained from the premises of the Federal University of Technology, Owerri, Nigeria on 5° 23' 3.04" N 6° 59' 37.08" E. They were confirmed by a plant taxonomist at the Forestry and Wildlife Technology Department, Federal University of Technology, Owerri, Nigeria, assigned the voucher number FUTO/FWT/ERB/2024/108 and deposited in their herbarium. Afterwards, samples were carefully sorted, washed under tap water, before sun-dried. They were then powdered and stored in stoppered plastic containers.<sup>22</sup> Aqueous extract of the leaf was prepared following the method of Akujobi et al.,<sup>23</sup> by weighing 107 g of powdered sample into 1500 mL of distilled water, in a 2000 mL conical flask. After boiling for 20 minutes, it was allowed to cool to room temperature before filtering with Whatman No. 1 filter paper. Determination of filtrate concentration was done in triplicate by completely evaporating 10 mL of filtrate to constant weight, using an

oven at 100 °C. The average weight per millilitre was calculated, and the filtrate was stored in a refrigerator at 4 °C.<sup>12</sup>

### Phytochemical screening of the extract

Quantitative phytochemical screening of the prepared *P. vaginatum* leaf extract was carried out using gas chromatography – mass spectrometry (GC-MS). The instrument (JEOL GCmate II GC/MS system, USA, Inc.) used had four double focusing mass analyzer. The HP 5Ms capillary column adopted had film thickness of 0.10 – 1.00 µm, made of (5%-Phenyl)-methylpolysiloxane. High purity helium was used as the carrier gas and was operated at a flow rate of 1 mL/min. The inlet and oven temperatures were maintained at 250°C and 50 to 250 °C at 10 °C/min, respectively. Also, the temperature of the MS transfer line was set at 250 °C. Analysis of the mass spectrum was carried out using electron impact ionization at 70 eV. The resulting data was assessed using total ion count (TIC) for compound identification and quantification. Then GC/MS database of spectra of known components was used to compare the spectra of the components obtained for identification.

### *Paspalum vaginatum* extract-mediated synthesis of zinc oxide nanoparticles

Zinc oxide nanoparticles used in this study were synthesized with aqueous *P. vaginatum* leaf extract, following the method of Amuthavalli et al.,<sup>13</sup> with slight modifications. The temperatures of 90 mL of 0.05 M zinc nitrate hexahydrate ( $\text{Zn}(\text{NO}_3)_2 \cdot 6\text{H}_2\text{O}$ ) and 10 mL *Paspalum vaginatum* extract, in separate flasks, were adjusted in a water bath (Model No.: DK420, Wincom, China) to 80 °C. Then the pH of the extract was adjusted to 10 by drop-wise addition of 1M NaOH solution. This was followed by reacting them for 30 minutes whilst continuously stirring at 80 °C. The resulting suspension was allowed at room temperature for 24 h for completion of biosynthesis. Changes in colour of the suspension were visually monitored during biosynthesis. After 24 h of synthesis, the resulting suspension was centrifuged (Model No.: C-802D Wincom Company Ltd., China) for 30 min at 5000 rpm to sediment the nanoparticles. The nanoparticles were washed three times by adding distilled water and centrifuging at 5000 rpm for 30 minutes. Then the ZnONPs were stored for further studies.

### Characterization of as-prepared zinc oxide nanoparticles

Resulting zinc oxide nanoparticles were characterized by analysing them using Fourier transform infrared (FTIR) spectroscopy (Model 5500 Compact FTIR by Agilent Technologies, USA) for the presence and types of functional groups in zinc oxide nanoparticles. This was done by uniformly dispersing and compressing the ZnO nanoparticles in matrices of dry KBr, to give transparent discs, which were used as a standard to scan the spectra between 4000–650  $\text{cm}^{-1}$ , at a resolution of 8  $\text{cm}^{-1}$ .<sup>12</sup> Guidelines of Sigma-Aldrich,<sup>24</sup> were followed to describe the appearances of peaks, functional groups, as well as compounds present in the ZnONPs. Ultraviolet-visible spectroscopy was done using Thermo Scientific, BioMate 3S, USA, to determine their absorbance spectrum, using a 2 mL quartz cuvette, at a resolution of 1 nm, with 1 cm path length, and 200–800 nm range.<sup>25</sup> X-ray diffraction was done using an X'pert PANANALYTICAL instrument to determine the phase composition, texture, and crystal structure or orientation of the ZnO nanoparticles. It was operated at a voltage of 40 kV and a current of 30 mA, with CuK ( $\alpha$ ) radiation.<sup>25</sup> ZnONPs crystalline size was determined according to Scherrer's formula shown in Equation 1;

$$L = \frac{k\lambda}{\beta \cos \theta} \quad 1$$

Where L refers to ZnONPs crystalline size,  $\beta$  refers to full width at half maximum (FWHM) of the most intense diffraction peak, detected to be 0.37,  $\theta$  refers to the diffraction angle (36.42), K refers to Scherrer's constant ( $K = 0.94$ ), and  $\lambda$  refers to the wavelength of X-ray (1.54178 Å). Transmission electron microscopy (TEM) using Jeol 200CX was done to determine the morphology and size of ZnO nanoparticles, and ImageJ software was used to analyse the obtained photomicrograph. The Malvern Zen 3600 (Zita Sizer) Instrument

Corps. UK was used to analyse the size distribution of ZnO nanoparticles in a solution.<sup>26</sup>

#### Assay of larvicidal activity of nanoparticles

##### Collection and rearing of test larvae

Mosquito larvae were collected from stagnant water in an open tank, at Ezioobodo, Imo State, Nigeria (5° 21' 34" N 7° 0' 23" E). Following standard identification keys by Gillet<sup>27</sup> and Oyerinde,<sup>28</sup> an expert entomologist at the Department of Animal and Environmental Biology, University of Port Harcourt, Nigeria, identified them as Instar IV larvae of the malarial vector, *Anopheles* sp. The larvae were kept in plastic enamel trays containing dechlorinated water and maintained continuously under standard insectary conditions (80 ± 10% relative humidity, 28 ± 1°C temperature, and 12 h light/12 h darkness photoperiod).<sup>29</sup> Feeding was done by adding glucose to the water, according to the feeding regime specified by Carvalho et al.<sup>30</sup> This was allowed for 24 h, to enable the larvae to acclimatize to the new environment.

##### Dose–response bioassay

Assay for larvicidal activity was carried out using 0.44, 0.22 and 0.11 g/L concentrations of synthesized zinc oxide nanoparticles in clean plastic containers. Twenty *Anopheles* sp larvae (instar IV) were separately exposed to each of 0.44, 0.22 and 0.11 g/L concentrations of ZnO nanoparticles. Control samples, which ran simultaneously with test experiments, were prepared without the addition of ZnO nanoparticles. The experiment was prepared in triplicate and maintained at room temperature, with a photoperiod of 16:8 hours light and dark cycle, without supplying food (Figure 1). The number of dead larvae (mortality) was counted at intervals of 1 h, until 26 h of exposure. A specimen was considered dead if, upon stimulation by touch, it either did not move at all or moved sluggishly and was unable to rise towards the surface of the rearing medium. The percentage mortality of the instar IV larva was calculated as described by Madanagopal et al.,<sup>31</sup> using the formula in Equation 2;

$$\text{Percentage mortality} = \frac{\text{Number of dead larvae}}{\text{Number of larvae introduced}} \times 100 \quad 2$$

Using regression analysis, the LC<sub>50</sub> value of ZnO nanoparticles was calculated.

##### Assay of antibacterial activity of synthesized ZnO nanoparticles

Assay of antibacterial activity of zinc oxide nanoparticles synthesized using the extract of *P. vaginatum* was carried out against clinical isolates of *Salmonella* spp. and *Escherichia coli*. Isolates were obtained from the Diagnosis Unit of the FUTO University Teaching Hospital, Owerri, Imo State, Nigeria. *Salmonella* spp. isolates were authenticated by sub-culturing on Salmonella-Shigella agar (SSA) and Xylose-Lysine-Deoxycholate agar (XLD, Oxoid, UK). Observation of red-pink colonies of about 2 to 3 mm in diameter, with black centres on XLD agar, and colourless colonies with black centres on SSA were considered positive for *S. spp.*<sup>32</sup> On the other hand, *E. coli* was authenticated on Eosin Methylene Blue (EMB) agar, and observation of metallic sheen colour with black centre was considered positive.<sup>33</sup> Antibacterial assay was carried out in duplicates, following the agar well diffusion method by Chauhan et al.,<sup>34</sup> with slight adjustments. Bacterial cultures were first rejuvenated by separately inoculating a loopful of each identified isolate into 5 mL of nutrient broth, followed by incubation at 37 °C for 24 h. Standardization of inocula was done by adjusting the turbidity of each culture to match 0.5 McFarland solution (~10<sup>8</sup> cfu/mL). Subsequently, prepared Mueller-Hinton (MH) agar plates were aseptically inoculated with 0.1 mL of each standardized test inoculum. Using a sterilized 1 cm cork borer, four wells each were dug into the Petri plates, and correspondingly filled with 53.3 µg/mL, 26.7 µg/mL and 13.3 µg/mL concentrations of ZnONPs. Ciprofloxacin disc and sterilized distilled water were applied as positive and negative controls, respectively. After plates were allowed to enable nanoparticles permeate the media, plates were incubated for 24 h at 37 °C. The degree of antibacterial activity was determined by measuring zones of inhibition, in millimetres, produced against each isolate.

##### Statistical analysis of results

Mean and standard deviations of all data generated from the triplicate measurements in this study, except for antibacterial analysis, which was duplicates, were determined by applying suitable tools in Minitab 17 software and Microsoft Excel 2010. Affected results were modelled using SigmaPlot 15.0 software.

## Results and Discussion

*Paspalum vaginatum* aqueous leaf extract used in this study had an average pH of 6.5±0.9, with an average concentration of 7.33±1.89 mg/mL.

##### Phytochemical contents of *Paspalum vaginatum* extract

From the chromatogram obtained in this study, the aqueous extract of *Paspalum vaginatum* was composed of ten (10) different compounds. These include hexadecanoic acid, methyl ester; n-Hexadecanoic acid; 9-Octadecenoic acid (Z)-, methyl ester; Oleic acid; Dodecanoic acid, 1-(hydroxymethyl)-1,2-ethanediyl ester; N-[4-Methoxy-6-(2,2,2-trifluoro-1-trifluoromethyl-ethoxy)-[1,3,5]triazin-2-yl]-benzene-1,4-diamine; Benzenamine,4-methoxy-N-(triphenylphosphoranylidene); 4-Nitrophenyl laurate; Dodecanoic acid, 1,2,3-propanetriyl ester; 4-Methoxy-3-nitrobenzyl alcohol. Details of the compounds are shown in Table 1. The pH of 6.5±0.9 recorded for *P. vaginatum* extract suggested that it is intrinsically slightly acidic. During bioreduction to form nanoparticles, the pH of the reacting medium is essential as it is capable of affecting the characteristics and activities of the resulting nanoparticles.<sup>35</sup> This was the reason for the adjustment of pH to alkaline before biosynthesis began. Results of this study also indicated that the extract contained appreciable diversity and concentrations of biomolecules/phytochemicals. These phytochemicals, including flavonoids, alkaloids, carbohydrates, proteins and amino acids, and phenolic compounds, which possess remarkable biological activity, are referred to as secondary metabolites. They are usually ubiquitous in plants and have been exploited in drug development.<sup>36</sup> A previous report has shown the presence of similar phytochemicals, including flavonoids, glycosides, alkaloids, terpenoids, saponins, volatile oils, triterpenoid esters, tannins, phytosterols, resins, reducing sugars, proteins, carbohydrates, and fixed oils in the extract of *P. vaginatum*.<sup>37</sup> The presence of these phytochemicals is essential for the reduction of metal ions into nanosized particles. This has been corroborated in a study by Nasir et al.,<sup>29</sup> which reported that plant secondary metabolites, including alkaloids, enzymes, proteins and amino acids, tannins, and flavonoids serve as reducing and capping agents for the bio-reduction of metal oxides to produce metal oxide nanoparticles. Surprisingly, there is a dearth of reports on phytochemical analysis of the extract of *P. vaginatum* using gas chromatography-mass spectrometry.

##### Visual observation of the synthesis of zinc oxide nanoparticles

During the synthesis of ZnONPs using *P. vaginatum* extract, it was observed that the colour of the extract changed from brown solution to dark-brown precipitate. The average concentration was 2.53±0.1 mg/mL. The observed change of the *P. vaginatum* extract solution from brown to dark-brown precipitate, on addition of zinc nitrate hexahydrate solution, signified the gradual reduction and capping of the metal oxide ions to metal oxide nanoparticles. Using leaf extracts of *Catharanthus roseus* (L.) to biosynthesize zinc oxide nanoparticles, similar change in colour of zinc salt from white to yellow, which was attributed to production of ZnO nanoparticles was also reported by Mishra et al.<sup>20</sup> On their part, our report is also similar to the observation of colour change from green to light-brown, coupled with the formation of precipitate, which confirmed synthesis of nanoparticles. After overnight drying, they obtained greenish-black coloured ZnO nanoparticles.<sup>3</sup>

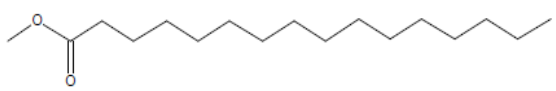
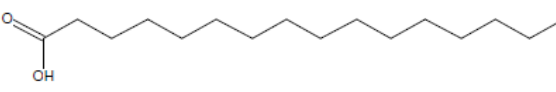

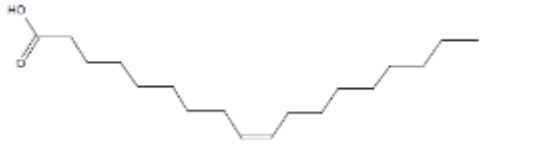
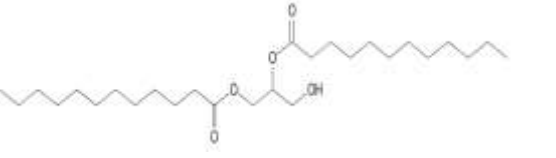
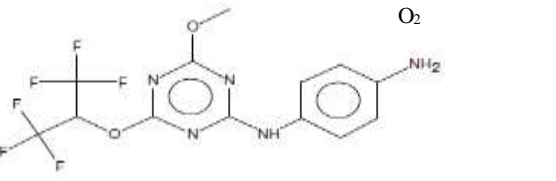
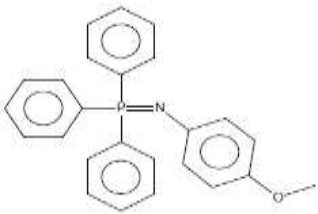
##### Characteristics of *P. vaginatum* extract-mediated ZnO nanoparticles

Figure 2 is the FTIR spectrum of the resulting ZnONPs, which indicates the formation of peaks. Table 2 shows the appearances of

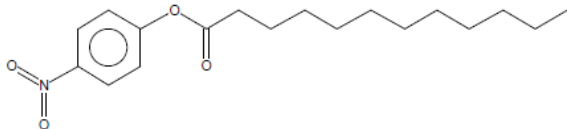
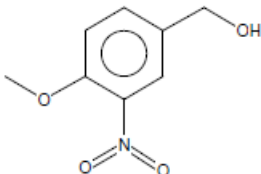
peaks, functional groups, and compounds present on the *P. vaginatum* extract-mediated zinc oxide nanoparticles. From the results of dynamic light scattering (DLS) analysis of resulting ZnONPs, the mean size was  $35.34 \pm 1.64$  nm, with a 0.63 polydispersity index. The XRD pattern of *P. vaginatum* extract-mediated ZnO nanoparticles showed that they were crystalline, with a hexagonal wurtzite structure. As shown in Figure 3, there were eleven peaks formed on the

spectrum, at  $2\theta$  of  $4.62^\circ$ ,  $9.02^\circ$ ,  $13.46^\circ$ ,  $31.92^\circ$ ,  $33.28^\circ$ ,  $34.62^\circ$ ,  $36.44^\circ$ ,  $47.64^\circ$ ,  $56.84^\circ$ ,  $63.02^\circ$  and  $68.16^\circ$ . The following peak positions and their corresponding orientation planes are  $31.92^\circ$  (100),  $34.62^\circ$  (002),  $36.44^\circ$  (101),  $47.64^\circ$  (102),  $56.84^\circ$  (110),  $63.3^\circ$  (200), and  $68.16^\circ$  (112). The estimated crystalline size of the nanoparticles was 23.6 nm, with JCPDS

**Table 1:** Details of compounds observed on chromatogram of *Paspalum vaginatum* extract

Peak No.	Retention Time (min)	% of Total	Identity of Compound	Chemical Structures	Molecular Formula	Molecular Weights
1	7.40	1.54	Hexadecanoic acid, methyl ester		$C_{17}H_{34}O_2$	270
2	7.69	3.27	n-Hexadecanoic acid		$C_{16}H_{32}O_2$	256
3	8.27	1.48	9-Octadecenoic acid (Z)-, methyl ester		$C_{19}H_{36}O_2$	296
4	8.54	5.03	Oleic acid		$C_{18}H_{34}O_2$	282
5	9.02	2.38,	Dodecanoic acid, 1-(hydroxymethyl)-1,2-ethanediyl ester		$C_{27}H_{52}O_5$	456
6	9.43	3.45	N-[4-Methoxy-6-(2,2,2-trifluoro-1-trifluoromethyl-ethoxy)-[1,3,5]triazin-2-yl]-benzene-1,4-diamine		$C_{13}H_{11}F_6N_5O_2$	383
7	9.78	6.76	Benzenamine, 4-methoxy-N-(triphenylphosphoranylidene)		$C_{25}H_{22}NOP$	383
8	10.70	7.18	4-Nitrophenyl laurate		$C_{18}H_{27}NO_4$	321



9	10.23	1.87	Dodecanoic acid, 1,2,3-propanetriyl ester		C <sub>39</sub> H <sub>74</sub> O <sub>6</sub>	638
10	14.94	1.01	4-Methoxy-3-nitrobenzyl alcohol		C <sub>8</sub> H <sub>9</sub> NO <sub>4</sub>	183



**Figure 1:** Cross-section of the setup for larvicidal bioassay of biosynthesized ZnONPs

No.: 04-005-5076. Figure 4 is the ultraviolet-visible absorbance spectrum of ZnO nanoparticles synthesized using *P. vaginatum* extract. It indicated an absorbance range of 293 nm to 336 nm, with a peak formed at 307 nm.

A micrograph of transmission electron microscopy of *P. vaginatum* extract-mediated ZnONPs is presented in Figure 5. It indicated the spherical shape, polydispersed, non-uniform sizes, and no agglomeration of pure synthesized ZnONPs. At 100 nm resolution, their sizes ranged from 0.52 nm to 8.32 nm, with a mean of  $3.96 \pm 2.4$  nm. The micrograph also revealed the light, darkest and dark parts which characterize nanoparticles. Fourier transform infrared spectrum reveals the presence and types of functional groups of phytochemicals, which were implicated in the formation of nanoparticles.<sup>12</sup> In this study, a range of functional groups was detected. Murugan et al.<sup>6</sup> had reported that functional groups, including carbonyl and hydroxyl of amines, flavonoids and other metabolites, react with metal ions and reduce them during nanoparticles biosynthesis. In their biosynthesized ZnONPs, Mishra et al.<sup>20</sup> reported the detection of a wide absorption peak at  $3328 \text{ cm}^{-1}$ , which signified stretching of -OH or phenolic groups, an absorption peak at  $547 \text{ cm}^{-1}$  corresponding to the characteristic Zn-O bond. Furthermore, the characteristics of peaks detected on ZnONPs biosynthesized in a related study were; a broad, strong peak at  $3413.5 \text{ cm}^{-1}$  representing hydroxyl (-OH-) group, a

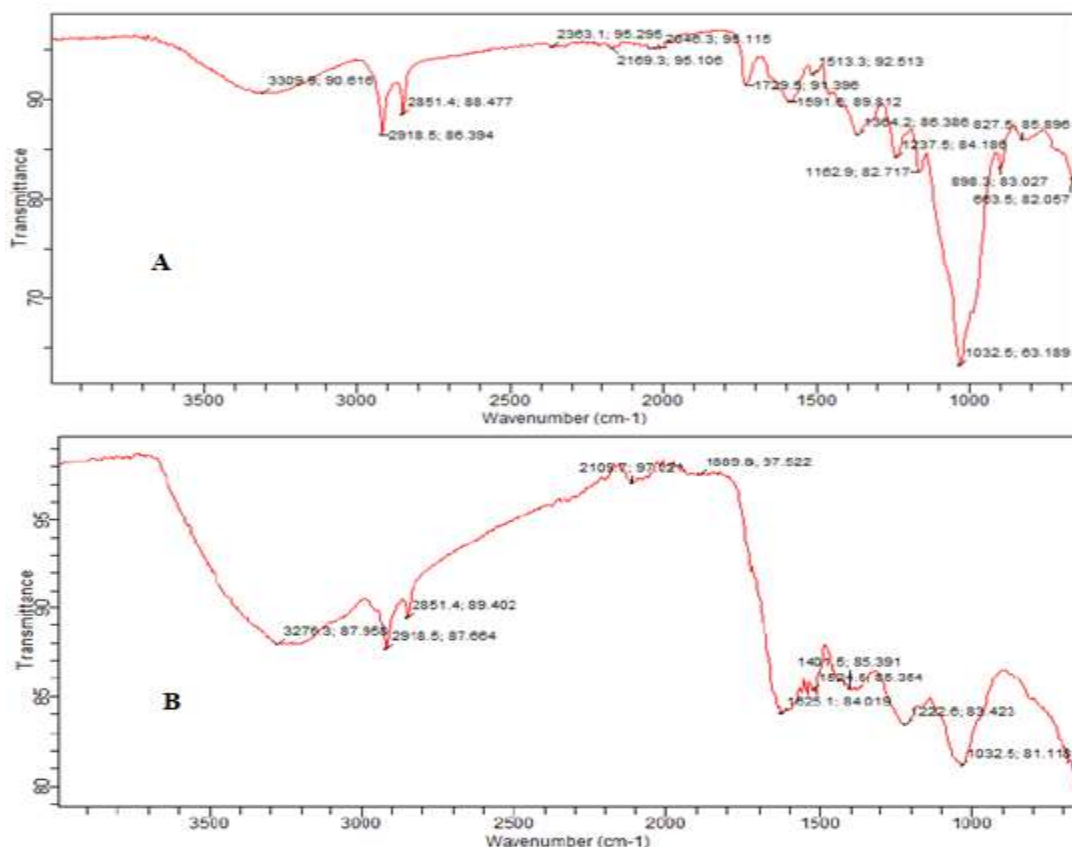
weak peak at  $2923.5 \text{ cm}^{-1}$  representing -CH<sub>3</sub>- of alkanes, a weak peak at  $2853.0 \text{ cm}^{-1}$  for -CH<sub>2</sub>- of alkanes, a strong at  $1629.5 \text{ cm}^{-1}$  for -CH=CHR- of aromatic, a weak peak at  $1501.9 \text{ cm}^{-1}$  for -N=O- of nitroso, a medium peak at  $1410.1 \text{ cm}^{-1}$  for -C-C- of aromatic, a strong peak at  $1053.1 \text{ cm}^{-1}$  for -C=O- stretch of alcohol, and a strong peak at  $485.9 \text{ cm}^{-1}$  for -C-H-wag of alkyl halides.<sup>3</sup> Badran et al.<sup>39</sup> had reported that nanoparticles with polydispersity index values below 0.3 are said to be monodispersed. Hence, ZnONPs obtained in this study are polydisperse. The intense and sharp peaks on the XRD spectrum obtained in this study indicated high crystallinity of the synthesized ZnONPs. The XRD spectrum is comparable to those reported in previous studies. The peaks and their corresponding planes were reported at  $2\theta = 31.76^\circ$  (100),  $34.42^\circ$  (002),  $36.24^\circ$  (101),  $47.53^\circ$  (102),  $56.59^\circ$  (110),  $62.86^\circ$  (103),  $66.38^\circ$  (200),  $67.94^\circ$  (112),  $69.08^\circ$  (201),  $72.56^\circ$  (004),  $76.92^\circ$  (202).<sup>13</sup> In another report, the peak angles and their corresponding lattice planes obtained from ZnO nanoparticles synthesized using extract of *Andrographis paniculata* were found at  $2\theta$  values of  $31.72^\circ$  (100),  $35.31^\circ$  (002),  $36.67^\circ$  (101),  $47.47^\circ$  (102),  $57.32^\circ$  (110),  $63.40^\circ$  (103), and  $69.36^\circ$  (112). With maximum crystalline intensity recorded at the lattice plane of 101, the size of the nanoparticles was estimated at 17.3 nm. The range and peak of UV-visible light absorption recorded in this study indicate that the ZnONPs can only be excited by UV rays. In some previous

studies, the peak of ultraviolet visible light absorption by zinc oxide nanoparticles was at 346 nm,<sup>15</sup> 360 nm,<sup>40</sup> 364 nm,<sup>13</sup>  $350 \pm 0.23$  nm,<sup>41</sup> which are slightly higher than 307 nm obtained in this study. Features of zinc oxide nanoparticles synthesized in this study, on the TEM micrograph, also matched those of previous studies. ZnONPs were quasi-spherical, with a diameter of about ~17 nm.<sup>3</sup> They were polydispersed, spherical-shaped and 49.21 - 65.43 nm in size.<sup>1</sup> Also,

Omeh et al.<sup>41</sup> had reported the synthesis of ZnONPs with particle size distribution of 49.75 nm and 0.519 polydispersity index (PDI). These values are considerably similar to the findings of the present study.

#### Larvicidal activity of synthesized ZnO nanoparticles

Results of larvicidal activities of different concentrations of resulting ZnONPs on instar IV larvae of *Anopheles* sp, studied for 26 h, are

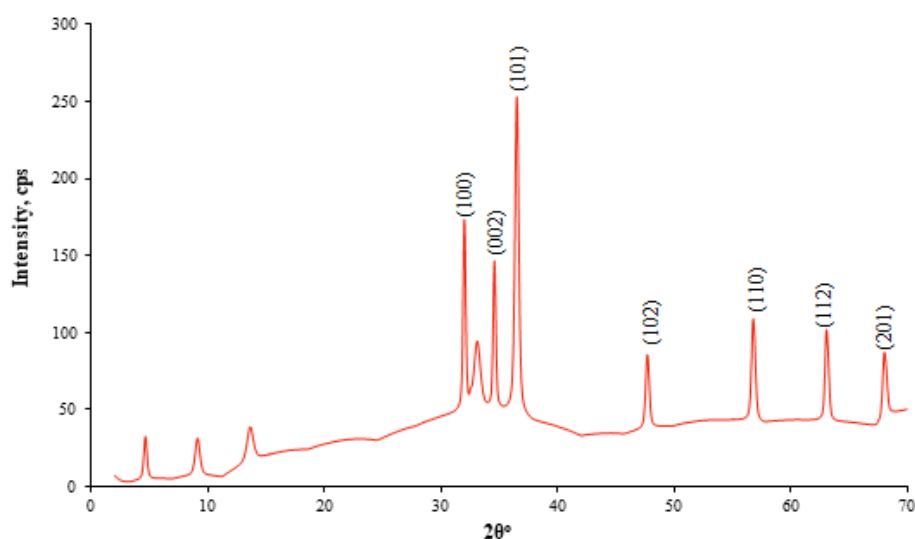


**Figure 2:** FTIR spectra of (A) *P. vaginatum* extract (B) *P. vaginatum* extract-mediated ZnONPs.

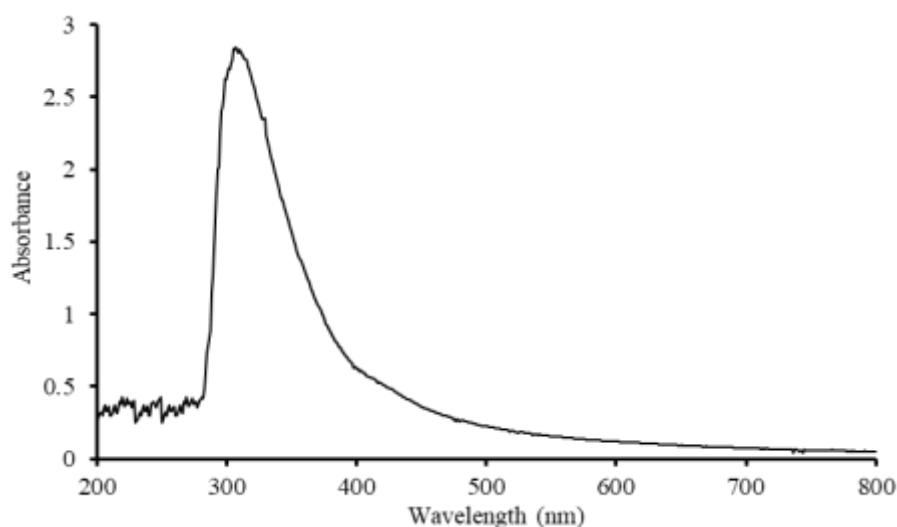
**Table 2:** FTIR peak assignment for the resulting ZnONPs.

Absorbance peak (cm <sup>-1</sup> )		Appearance	Functional group	Compound present
<i>P. vaginatum</i> extract	<i>P. vaginatum</i> extract-mediated ZnONPs			
1032.5	1032.5	Strong	S=O stretching	Sulfoxide
1162.9		Medium		
1237.5		Medium		
	1222.6	Strong	C-O stretching	Alkyl aryl ether
1364.2		Medium		
	1401.5	Strong	S=O stretching	Sulfonyl chloride
1513.3	1524.5	Strong	N-O stretching	Nitro compound
1591.6		Weak	C=C stretching	Aromatic

			C=C stretching	Conjugated alkene
	1625.1	Strong		Amine
			N-H bending	
1729.5		Weak	C=O stretching	Aldehyde
	1889.8	Weak	C-H bending	Aromatic compound
2169.3	2109.7	Weak	C≡C stretching	Alkyne
2851.4	2851.4	Strong	C-H stretching	Alkane
2918.5	2918.5	Strong	N-H stretching	Amine salt
		Strong	O-H stretching	Alcohol (intermolecular bonded)
3276.3	3276.3			
		Strong	C-H stretching	Alkyne
3309.9		Medium	N-H stretching	Secondary amine



**Figure 3:** XRD spectrum of *P. vaginatum* extract-mediated ZnONPs.



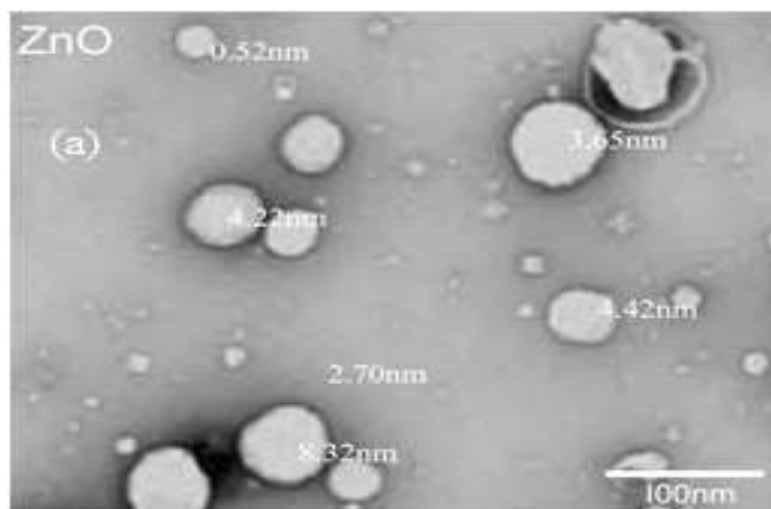
**Figure 4:** Ultraviolet visible absorbance spectrum of *P. vaginatum* extract-mediated ZnONPs

presented in Figure 6. These indicated that ZnONPs produced a time and dose-dependent relationship with percentage mortality. At 0.44 g/L of ZnONPs, it was observed that percentage mortality was

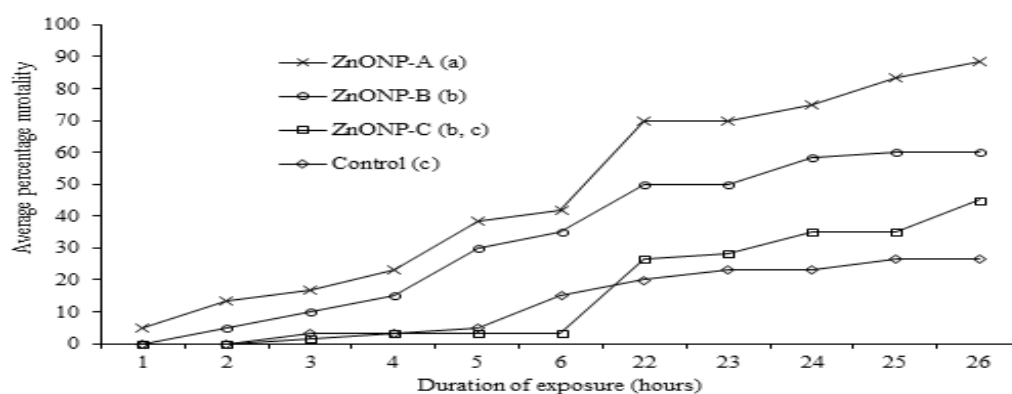
5.0±4.1% after 1 h of exposure, 41.7±4.1% after 6 h, and 88.3±0.0% after 26 h. At 0.22 g/L of ZnONPs, percentage mortality reduced to 0.0±0.0% after 1 h of exposure, 35.0±2.4% after 6 h, and 60.0±2.4%

after 26 h. At a concentration of 0.11 g/L, percentage mortality further reduced to  $0.0 \pm 0.0\%$  after 1 h,  $3.3 \pm 2.4\%$  after 6 h, and  $45.0 \pm 0.0\%$  after 26 h of exposure to ZnONPs. Comparatively, the percentage mortality recorded in ZnONPs-treated samples was higher than that recorded in control samples, with  $0.0 \pm 0.0\%$  at 1 h,  $15.0 \pm 0.8\%$  at 6 h, and  $26.7 \pm 2.5\%$  at 26 h. The median lethal concentration ( $LC_{50}$ ) of *P.*

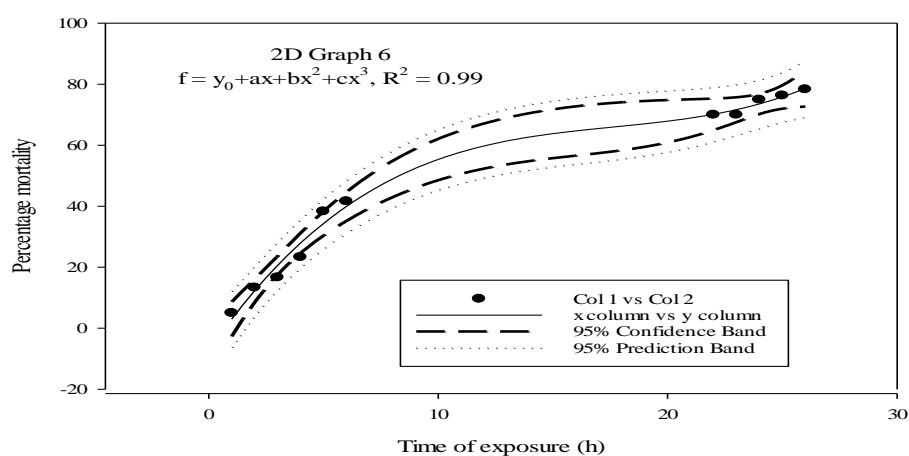
*vaginatum* extract-mediated ZnONPs samples, on Instar IV larvae of *Anopheles* sp. for 26 h, was found to be  $766.67 \pm 75.4$  mg/L. Results ( $\alpha = 0.05$ ) showed that percentage mortality at 0.44 g/L is significantly higher than those recorded at other concentrations, as well as in the control sample. Also, the percentage mortality at 0.22 mg/mL concentration of ZnONPs was significantly different from that of the



**Figure 5:** Transmission electron micrograph of *P. vaginatum* extract-mediated ZnONPs, at 100 nm resolutions.

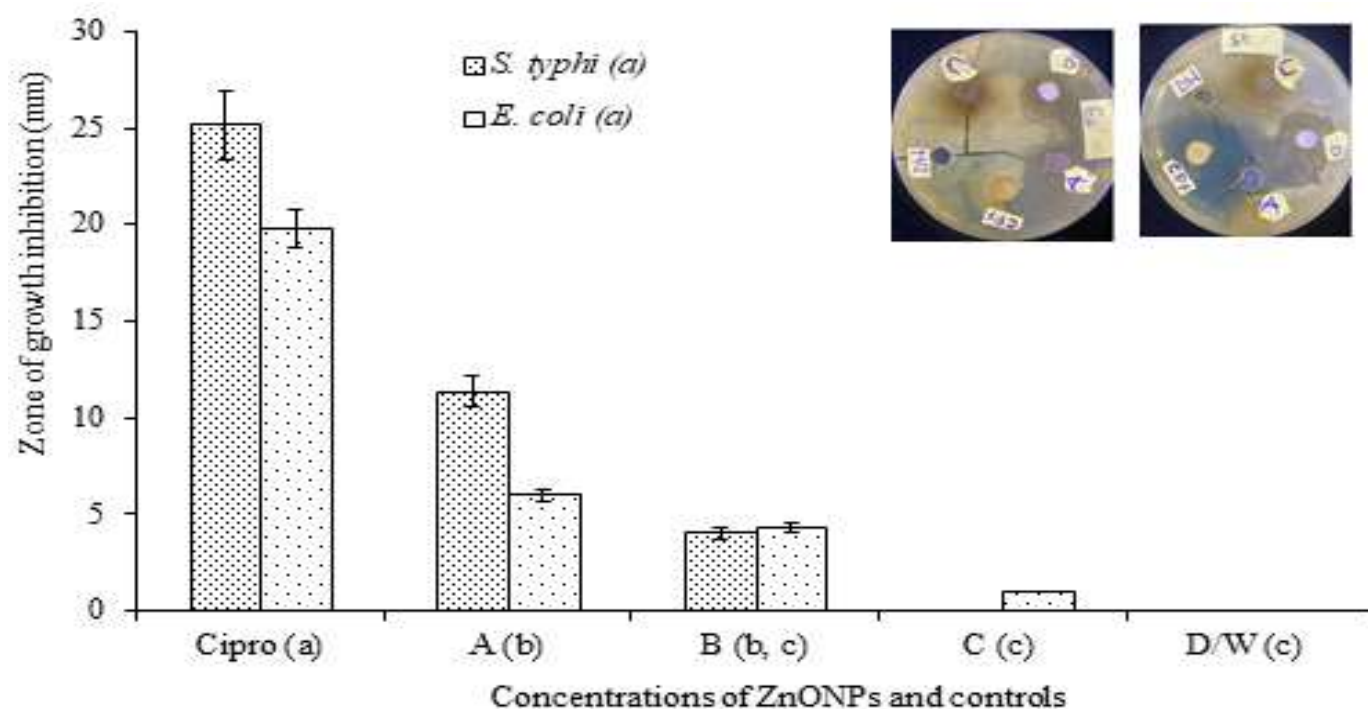


**Figure 6:** Percentage mortality of Instar IV anopheles mosquito larvae at different concentrations of ZnONPs (A, B and C = 0.44, 0.22 and 0.11 g/L concentrations respectively). Samples with similar letters, in parenthesis, are not significantly different ( $\alpha = 0.05$ ).



**Figure 7:** Sigmoidal, sigmoid, 5 parameter chart model of percentage mortality of Instar IV *Anopheles* mosquito larva by synthesized ZnONPs.





**Figure 8:** Bacterial growth inhibition of *S. sp.* and *E. coli* by synthesized ZnO nanoparticles, at different concentrations (A = 53.3 µg/mL, B = 26.7 µg/mL, C = 13.3 µg/mL and D/W = distilled water). Samples with similar lower case letters, in parenthesis, are not significantly different.

control sample and 0.44 g/L concentration. The percentage mortality in control samples was significantly different from those recorded at other concentrations of ZnONPs, except at 0.11 g/L concentration. When the resulting percentage mortality was modelled, it revealed that larvicidal activity of ZnONPs, at 0.44 g/L concentration, followed the polynomial, cubic equation (Equation 3);

$$f = y_0 + ax + bx^2 + cx^3, \text{ with } R^2 = 0.99; \quad 3$$

where  $f$  is the percentage mortality,  $x$  is time of exposure (h),  $y_0 = -7.44$ ,  $a = 10.98$ ,  $b = -0.58$  and  $c = 0.01$ . The resulting model chart is presented in Figure 7. The larvicidal activity obtained in this study was an indication that the synthesized ZnONPs were toxic to mosquito larvae. The significantly higher activity recorded in this study, at 0.44 g/L concentration of ZnONPs, implied that increase in concentrations of the nanoparticles was necessary for higher larvicidal activity on the test mosquito larvae. The dose and time-dependent larvicidal activities observed in this study were consistent with reports of previous studies, including Rather et al.<sup>15</sup> Results obtained by Dwivedi and Singh<sup>3</sup> revealed that mortality percentages and concentrations of synthesized ZnONPs were  $11.56 \pm 0.11\%$  at 200 ppm,  $19.47 \pm 1.10\%$  at 300 ppm, and  $28.76 \pm 2.40\%$  at 500 ppm after 24 h of exposure. Also,  $31.75 \pm 2.23$  ppm and  $189.56 \pm 2.44$  ppm were the recorded  $LC_{50}$  and  $LC_{90}$  values, respectively, at 24 h of exposure. In another study, percentage mortalities on *Aedes albopictus* were  $26.6 \pm 0.5\%$ ,  $43.3 \pm 0.5\%$ ,  $76.6 \pm 1.15\%$ ,  $93.3 \pm 0.57\%$ , and  $100 \pm 0.0\%$  at 80 mg/L, 100 mg/L, 120 mg/L, 140 mg/L and 160 mg/L of ZnO nanoparticles respectively. The  $LC_{50}$  and  $LC_{90}$  were 118 (105.1-125.08) mg/L and 135 (127.9-151.98) mg/L, respectively.<sup>15</sup> Also, at concentrations of 25 ppm, 50 ppm, 100 ppm, 150 ppm and 250 ppm of ZnO nanoparticles synthesized using the extract of *Cuscuta reflexa*, another study found that the percentages of mortality recorded on instar IV larvae of *An. stephensi* larvae were 30%, 50%, 60%, 70%, and 80% respectively. The resulting probit equation was  $y = 0.3969x - 11.641$ , with the  $LC_{50}$  value of  $50 \pm 0.12$ .<sup>40</sup> Benelli et al.<sup>42</sup> had revealed that ZnONPs are toxic to mosquito larvae because they inflict severe histological and morphological abnormalities, such as accumulation of zinc nanoparticles in the thorax and abdomen of larvae, alteration of their thorax shape, shrinkage of abdominal region, loss of anal gills, lateral hairs, and brushes, as well as damages to their midgut.

#### Antibacterial activity of synthesized ZnO nanoparticles

Synthesized ZnO nanoparticles produced appreciable dose-dependent activities against the bacterial isolates studied. Figure 8 is the antibacterial activity of zinc oxide nanoparticles synthesized in this study, using *P. vaginatum* extract. It indicated that synthesized ZnO nanoparticles recorded  $11.33 \pm 7.2$  and  $6.0 \pm 2.2$  mm bacterial growth inhibitions at 53.3 mg/mL concentration;  $4.0 \pm 2.2$  mm and  $4.33 \pm 1.3$  mm growth inhibitions at 26.7 µg/mL concentration; and  $0.0 \pm 0.0$  mm and  $1.0 \pm 1.41$  mm inhibitions at 13.3 µg/mL concentration, against *S. sp.* and *E. coli*, respectively. At lower concentrations, *E. coli* showed higher sensitivity than *S. spp.* Ciprofloxacin produced the highest growth inhibitions of 25.1 mm and  $19.78 \pm 3.8$  mm against *S. sp.* and *E. coli*, respectively. There was no recorded growth inhibition in samples tested with distilled water (negative control). Statistical analysis revealed that at  $\alpha = 0.05$ , there was no significant difference in the sensitivities of both bacterial isolates to different concentrations of ZnO nanoparticles. Also, the activity of ciprofloxacin was significantly higher than that of the ZnO nanoparticle concentrations used in this study. Comparatively, antibacterial activity recorded at 53.3 µg/mL concentration of ZnONPs was significantly higher than those recorded at 13.3 µg/mL concentration, and with distilled water. Results obtained in this study indicated that the *P. vaginatum* extract-mediated zinc oxide nanoparticles possessed considerable antibacterial activity against *E. coli* and *S. spp.* It recorded higher activities at higher concentrations of nanoparticles. A previous study had reported that ZnO nanoparticles synthesized using *Lawsonia inermis* extract inhibited the growth of pathogenic bacterial isolates, and recorded 13.3 mm growth inhibition against *E. coli* and 8.4 mm against *B. subtilis*.<sup>13</sup> ZnONPs synthesized using pineapple peel extract demonstrated antibacterial activity against *B. subtilis*, but no activity against *Salmonella enterica* serotype Choleraesuis. It recorded 8.67 to 9.67 mm, 13.33 to 15.0 mm, and 11.0 to 12.33 mm growth inhibition against *B. subtilis*, at 1%, 3% and 5% of ZnO nanoparticles, respectively.<sup>43</sup> However, our observation of a dose-dependent activity in this study was at variance with the report of Basri et al.<sup>43</sup> which observed declining activity with an increase in concentration of ZnONPs. They attributed their observation to the susceptibility of *B. subtilis* toward a limited specific concentration of ZnO NPs, which

resulted in a reduction in activity with further increase in concentration to 5%. They concluded that Gram-positive bacterial isolates showed more sensitivity to the synthesized ZnO nanoparticles than Gram-negative bacterial isolates.<sup>43</sup> Antibacterial potential of ZnO nanoparticles has been attributed to their capability to disrupt the cell wall of pathogens, reduce their cell surface hydrophobicity and down-regulation of oxidative stress-resistance genes, which result in degradation and cell death.<sup>44,45</sup>

## Conclusion

To contribute to the sustenance of the biological method of nanoparticles synthesis, aqueous extract of *P. vaginatum* was used to synthesize zinc oxide nanoparticles. XRD spectrum revealed the crystalline nature and hexagonal wurtzite structure of synthesized ZnONPs. From the micrograph, the nanoparticles are spherical, with a mean size of  $3.96 \pm 2.4$  nm. There was considerable dose and time-dependent larvicidal activity of synthesized ZnONPs against instar IV *Anopheles* sp larvae, with  $88.3 \pm 0.0\%$  mortality recorded after 26 h of exposure. Synthesized ZnONPs produced  $11.33 \pm 7.2$  mm and  $6.0 \pm 2.2$  mm growth inhibitions against *Salmonella* sp. and *Escherichia coli*, respectively, at  $53.3 \mu\text{g/mL}$  concentration. This study has demonstrated that *P. vaginatum* aqueous extract is suitable for the synthesis of ZnONPs, with reasonable antibacterial and larvicidal activities. As nanotechnology keeps growing, it is essential to guarantee its sustainability. Therefore, further studies should be carried out using *P. vaginatum* extract to synthesize other types of nanoparticles. There is a need to optimize the effects of relevant parameters that affect the properties of the resulting nanoparticles. Although bulk zinc oxide is approved for industrial use, the toxicological analysis of zinc oxide nanoparticles is recommended to better understand their effects on humans and the environment. This will further encourage its wider applications.

## Conflict of Interest

The authors declare no conflict of interest.

## Authors' Declaration

The authors hereby declare that the work presented in this article is original and that any liability for claims relating to the content of this article will be borne by them.

## Acknowledgements

The Authors appreciate the Heads of the Department of Biotechnology, Department of Biology, and Department of Microbiology, Federal University of Technology, Owerri, Nigeria, for access to their laboratories and equipment during this study. The authors did not receive funding from any government or private organization for this study.

## References

- Ramkumar G, Shivakumar MS, Alshehri MA, Panneerselvam C, Sayed S. Larvicidal potential of *Cipadessa baccifera* leaf extract-synthesized zinc nanoparticles against three major mosquito vectors. *Green Proc. and Synth.* 2022; 11: 757-765.
- World Health Organization. Preventive action is vital to curtail dengue outbreaks in Sri Lanka. [cited 2025 Nov 17]. Available from: <https://www.who.int/srilanka/news/detail/08-07-2019-preventive-action-is-vital-to-curtaildengue-outbreaks-in-sri-lanka>.
- Dwivedi MK Singh PK. *In vitro* larvicidal, antioxidant, and DNA binding activity of biosynthesized zinc oxide nanoparticles conjugated with *Andrographis paniculata* aqueous extract. *Indian J. Biochem. & Biophys.* 2023; 60: 611-623.
- Bharathidasan M, Kotra V, Abbas SA, Mathews A. Review on biologically active natural insecticides from Malaysian tropical plants against *Aedes aegypti* and *Aedes albopictus*. *Arabian J. Chem.* 2024; 17(105345): 1-10. <https://doi.org/10.1016/j.arabjc.2023.105345>
- Carson J, Erriah E, Herodotou S, Shtukenberg AG, Smith L, Ryazanskaya S, Ward MD, Kahr B, Lees RS. Overcoming insecticide resistance in *Anopheles* mosquitoes by using faster-acting solid forms of deltamethrin. *Malaria Journal*, 22(129) 1-8 (2023) <https://doi.org/10.1186/s12936-023-04554-x>
- Murugan K, Panneerselvam C, Subramaniam J, Paulpandi M, Rajaganesh R, Vasanthakumaran M. Synthesis of new series of quinoline derivatives with insecticidal effects on larval vectors of malaria and dengue diseases. *Sci. Rep.* 2022; 12(1): 1-11.
- Pittarate S, Rajula J, Rahman A, Vivekanandhan P, Thungrabeab M, Mekchay S. Insecticidal effect of zinc oxide nanoparticles against *Spodoptera frugiperda* under laboratory conditions. *Insects* 2021; 12(11): 1017.
- Asthana N, Pal K, Aljabali AA, Tambuwala MM, de Souza FG, Pandey K. Polyvinyl alcohol (PVA) mixed green-clay and *Aloe vera* based polymeric membrane optimization: Peel-off mask formulation for skin care cosmeceuticals in green nanotechnology. *J. Mol. Struct.* 2021; 1229: 129592.
- Suparna R. Anantharaman P. Biosynthesis of silver nanoparticles by *Chaetomorpha antennina* (Bory de Saint-Vincent) Kutzing with its antibacterial activity and ecological implication. *J. Nanomed. and Nanotech.* 2017; 8(5): 1-9.
- Shehata AZI, Labib RM, Abdel-Samad MRK. Insecticidal activity and phytochemical analysis of *Pyrus communis* L. extracts against malarial vector, *Anopheles pharoensis* Theobald, 1901 (Diptera: Culicidae). *Polish J. Entomol.* 2021; 90(4): 209-222.
- Rouhi J, Mahmud S, Naderi N, Ooi CR, Mahmood MR. Physical properties of fish gelatin-based bio-nanocomposite films incorporated with ZnO nanorods. *Nanoscale Res. Lett.* 2013; 8: 364.
- Anuforo HU, Ogbulie TE, Udebuani AC, Ezeji EU. Synthesis of zinc oxide nanoparticles using extract of *Paspalum vaginatum* and assessment of their biological activity against *Staphylococcus aureus* and *Escherichia coli*. *UMYU J. Microb. Res.* 2023; 8(2): 1-11.
- Amuthavalli P, Hwang J, Dahms H, Wang L, Anitha J, Vasanthakumaran M, Gandhi AD, Murugan K, Subramaniam J, Paulpandi M, Chandramohan B, Singh S. Zinc oxide nanoparticles using plant *Lawsonia inermis* and their mosquitocidal, antimicrobial, anticancer applications showing moderate side effects. *Sci. Rep.* 2021; 11(8837): 1-13.
- Bhattacharya P, Chatterjee K, Swarnakar S, Banerjee S. Green synthesis of zinc oxide nanoparticles via algal route and its action on cancerous cells and pathogenic microbes. *Adv. Nano Res.* 2020; 3(1): 15-27.
- Rather GA, Nanda A, Ezhumalai P. Mosquito larvicidal activity of ZnO nanoparticles against dengue causing vector *Aedes albopictus* Using Leaf Extract of *Lavandula angustifolia*. *J. Nanostruct.* 2022; 12(3): 625-632.
- Oudhia A, Kulkarni P, Sharma S. Green synthesis of ZnO nanotubes for bioapplications. *International J. Curr. Eng. and Technol.* 2015; 1: 280-281.
- Saranya S, Eswari A, Gayathri E, Eswari S, Vijayarani K. Green synthesis of metallic nanoparticles using aqueous plant extract and their antibacterial activity. *Int. J. Curr. Microbiol. and Appl. Sc.* 2017; 6: 1834-1845.
- Devi RS, Gayathri R. Green synthesis of zinc oxide nanoparticles by using *Hibiscus rosa-sinensis*. *Int. J. Curr. Eng. and Technol.* 2014; 4: 2444-2446.
- Sangeetha G, Rajeshwari S, Venkatesh R. Green synthesis of zinc oxide nanoparticles by *Aloe barbadensis* miller leaf extract: Structure and optical properties. *Mat. Res. Bull.* 2011; 46: 2560-2566.
- Mishra D, Chitara MK, Negi S, Singh JP, Kumar R, Chaturvedi P. Biosynthesis of zinc oxide nanoparticles via leaf extracts of *Catharanthus roseus* (L.) G. Don and their application in improving seed germination potential and seedling vigor of *Eleusine coracana* (L.) Gaertn. *Adv. Agric.* 2023; 7412714: 1-11.
- Sulastri, Ahmad A, Karim A, Wahid I, Rauf W, Karim H, Farid AM. Green synthesized zinc oxide nanoparticles from *Coffea arabica*: bioprospecting and functional potential as an

- antioxidant and larvicide agent against *Aedes aegypti*. Trop J Nat Prod Res. 2025; 9(1): 90 – 96. <https://doi.org/10.26538/tjnpr/v9i1.13>
22. Opara FN, Anuforo HU, Okechukwu RI, Mgbemena IC, Akujobi CO, Adjeroh A. Preliminary phytochemical screening and antibacterial activities of leaf extracts of *Terminalia catappa*. J. Emerg. Trends in Eng. and Appl. Sc. 2012; 3(3): 424-428.
  23. Akujobi CO, Anuforo HU, Okereke JN, Ibeh C, Agbo CJ. Parametric optimization of synthesis of silver nanoparticles from *Mangifera indica* and *Prunus dulcis* extracts and their antibacterial activity. Analele Universității din Oradea, Fascicula Biologie 2020; 27(1), 21-26.
  24. Sigma-Aldrich. IR spectrum table and chart. [cited 2023 Sep 19]. Available from: <https://www.sigmaaldrich.com/NG/en/technical-documents/technical-article/analytical-chemistry/photometry-and-reflectometry/ir-spectrum-table>.
  25. Erdogan O, Abbak M, Demirbolat GM, Birtokocak F, Aksel M, Pasa S, Cevik O. Green synthesis of silver nanoparticles via *Cynara scolymus* leaf extracts: The characterization, anticancer potential with photodynamic therapy in MCF7 cells. PLoS ONE 2019; 14(6): 1-15.
  26. Amini N, Amin G, Jafari AZ. Green synthesis of silver nanoparticles using *Avena sativa* L. extract. Nanomed. Res. J. 2017; 2(1): 57-63.
  27. Gillet JD. Common African mosquitoes and their medical importance. London, UK: William Heinemann Medical Books Limited; 1972.
  28. Oyerinde JPO. Essentials of tropical medical parasitology. Akoka, Lagos: University of Lagos Press.; 1999.
  29. Nasir S, Usman M, Iqbal K, Ishaq M, Batool A, Arshad W. A novel ecofriendly control of arboviruses vectors (*Aedes aegypti* and *Ae. albopictus*) using *Trachyspermum ammi* seed extract-mediated silver nanoparticles (AgNPs). Mat. Proc. 2023; 4: 1-4.
  30. Carvalho DO, Nimmo D, Naish N, McKemey AR, Gray P, Wilke ABB, Capurro ML. Mass production of genetically modified *Aedes aegypti* for field releases in Brazil. J. Visualized Exp. 2014; 83: 1-10.
  31. Madanagopal N, Mahalingam L, Palanisamy S, Chandran S. Effect of phyto-synthesized silver nanoparticles on developmental stages of malaria vector, *Anopheles stephensi* and dengue vector, *Aedes aegypti*. Egyptian J. Basic and App. Sc. 2017; 4(3): 212-218.
  32. Abdul S, Ferhat A, Zunera T, Zafar A, Irshad A, Simon GP, Nighat N, Muhammad TA, Abdul R, Asadullah A, Irfan SS, MN, Olena P, Mohammad ZM. Prevalence of *Salmonella* spp. in chicken meat from Quetta retail outlets and typing through multiplex PCR. Rom. Biotechnol. Lett. 2019; 24(2): 271-279.
  33. American Society for Microbiology (ASM). Eosin-methylene blue agar plates protocols. [cited 2024 Jan 14]. Available from: <https://asm.org/protocols/eosin-methylene-blue-agar-plates-protocol#:~:text=EMB%20agar%20is%20also%20used,gram%20Dnegative%20bacteria%20appear%20pink>.
  34. Chauhan A, Verma R, Kumari S, Sharma A, Shandilya P, Li X, Battoo KM, Kumar R. Photocatalytic dye degradation and antimicrobial activities of pure and Ag-doped ZnO using *Cannabis sativa* leaf extract. Sci. Rep. 2020; 10(7881): 1-16.
  35. Malik R, Kousar, S. Plant-based synthesis of nanoparticles and applications. Journal of Xi'an Shiyou University, Nat. Sc. Ed. 2023; 19(17): 1-17.
  36. Dutt R, Garg V, Khatri N, Madan AK. Phytochemicals in anticancer drug development. Anti-Cancer Agents in Med. Chem. 2019; 19(2): 172-183.
  37. Al-Snafi PDAE. A review on chemical constituents and pharmacological activities of *Coriandrum sativum*. IOSR J. Pharm. 2016; 6(7): 17-42.
  38. Murugan K, Roni M, Panneerselvam C, Aziz A, Suresh U, Rajaganes R, Aruliah R, Mahyoub JA, Trivedi S, Rehman H, Al-Aoh, HAN, Kumar S, Higuchi A, Vaseeharan B, Wei H, Sethil-Nathan S, Canale A, Benelli G. *Sargassum wightii*-synthesized ZnO nanoparticles reduce the fitness and reproduction of the malaria vector *Anopheles stephensi* and cotton bollworm *Helicoverpa armigera*. Physiol. and Mol. Plant Path. 2018; 101: 202-213.
  39. Badran M. Formulation and *in vitro* evaluation of flufenamic acid loaded deformable liposomes for improved skin delivery. Digest J Nanomat. and Biostruct. 2014; 9: 1-12.
  40. Soni N, Dhiman RC. Larvicidal activity of zinc oxide and titanium dioxide nanoparticles synthesis using *Cuscuta reflexa* extract against malaria vector (*Anopheles stephensi*). Egyptian J. Basic and Appl. Sc. 2020; 7(1): 342-352.
  41. Omeh RC, Ali IJ, Adonu CC, Ogbonna JI, Ugorji LO, Mbah CC, Ugwu CO, Asogwa FK, Omeh AA, Ikeh GO, Mommoh AM, Onunkwo GC. Green synthesis of zinc oxide nanoparticles characterization and use for formulation of sunscreen topical creams. Trop. J. Nat. Prod. Res., 2025; 9(6): 2384 - 2394. <https://doi.org/10.26538/tjnpr/v9i6.5>
  42. Benelli G. Mode of action of nanoparticles against insects. Env. Sc.Pol. Res. 2018; 25(13): 12329-12341.
  43. Basri HH, Talib RA, Sukor R, Othman SH, Arifin H. Effect of synthesis temperature on the size of ZnO nanoparticles derived from pineapple peel extract and antibacterial activity of ZnO–starch nanocomposite films. Nanomat. 2020; 10(1061): 1-15.
  44. Kalra K, Chhabra V, Prasad N. Antibacterial activities of zinc oxide nanoparticles: A mini review. J. Phys.: Conf. Ser. 2022; 2267(012049): 1-12. <https://doi.org/10.1088/1742-6596/2267/1/012049>.
  45. Al-Mashhadani TA, Kadhum FM, Jawad AA, Ajeel KK, Mohsen AH. Investigating the antibacterial activity of zinc oxide nanoparticles against *Staphylococcus aureus* isolates. J. Biosci. Appl. Res., 2025; 11(1): 270-280. <https://doi.org/10.21608/jbaar.2025.419993>